



Leaf vein xylem conduit diameter influences susceptibility to embolism and hydraulic decline

Christine Scoffoni^{1,2}, Caetano Albuquerque³, Craig R. Brodersen⁴, Shatara V. Townes¹, Grace P. John¹, Hervé Cochard⁵, Thomas N. Buckley⁶, Andrew J. McElrone^{3,7} and Lawren Sack¹

¹Department of Ecology and Evolutionary Biology, University of California Los Angeles, 621 Charles E. Young Drive South, Los Angeles, CA 90095, USA; ²Department of Biology, Utah State University, Logan, UT 84322, USA; ³Department of Viticulture and Enology, University of California, Davis, CA 95616, USA; ⁴School of Forestry & Environmental Studies, Yale University, 195 Prospect Street, New Haven, CT 06511, USA; ⁵PIAF, INRA, Univ. Clermont-Auvergne, Clermont-Ferrand 63100, France; ⁶Plant Breeding Institute, Faculty of Agriculture and Environment, The University of Sydney, 12656 Newell Hwy, Narrabri, NSW 2390, Australia; ⁷USDA-Agricultural Research Service, Davis, CA 95616, USA

Summary

Author for correspondence:
Christine Scoffoni
Tel: +1 310 206 2887
Email: cscoffoni@ucla.edu

Received: 19 July 2016
Accepted: 10 September 2016

New Phytologist (2017) **213**: 1076–1092
doi: 10.1111/nph.14256

Key words: cavitation, microCT, percentage loss of conductivity, venation architecture, xylem collapse.

- Ecosystems worldwide are facing increasingly severe and prolonged droughts during which hydraulic failure from drought-induced embolism can lead to organ or whole plant death. Understanding the determinants of xylem failure across species is especially critical in leaves, the engines of plant growth.
- If the vulnerability segmentation hypothesis holds within leaves, higher order veins that are most terminal in the plant hydraulic system should be more susceptible to embolism to protect the rest of the water transport system. Increased vulnerability in the higher order veins would also be consistent with these experiencing the greatest tensions in the plant xylem network.
- To test this hypothesis, we combined X-ray micro-computed tomography imaging, hydraulic experiments, cross-sectional anatomy and 3D physiological modelling to investigate how embolisms spread throughout petioles and vein orders during leaf dehydration in relation to conduit dimensions.
- Decline of leaf xylem hydraulic conductance (K_x) during dehydration was driven by embolism initiating in petioles and midribs across all species, and K_x vulnerability was strongly correlated with petiole and midrib conduit dimensions. Our simulations showed no significant impact of conduit collapse on K_x decline. We found xylem conduit dimensions play a major role in determining the susceptibility of the leaf water transport system during strong leaf dehydration.

Introduction

Water transport from roots to leaves occurs through a network of xylem conduits, and because water is under tension, the system is subject to threat of failure. During drought, the tension in the xylem sap increases and can cause gas bubbles to expand and embolize xylem conduits, obstructing water movement. This phenomenon was one of the first observations in experimental biology: Probably therefore, these air bubbles, when in the sap vessels, do stop the free ascent of the water, as is the case of little portions of air got between the water in capillary glass tubes' (Hales, 1727). Given the increasing frequency and severity of drought events around the world (Sheffield & Wood, 2008), understanding species vulnerability to drought-induced embolism is critical. An efficient water supply through the xylem is fundamental to plant growth and survival, as leaves constantly need to replenish the water lost due to transpiration from open stomata when soil is moist, or from the cuticle and leaky stomata under prolonged intense drought. Leaves represent an especially important bottleneck in plants, accounting for at least 30% of the plant hydraulic resistance (Sack *et al.*, 2003). Leaf vein and

petiole embolism could thus represent a major constraint on plant function.

Water transport through leaves depends on two pathways that operate in series. First, water flows through the xylem in petiole and the major veins (i.e. midrib, second and third-order veins, also known as 'lower-order veins') and the minor veins (i.e. fourth- and higher order veins). Next, water flows through outside-xylem tissues including vascular parenchyma, bundle sheath and mesophyll cells. Both pathways are thought to contribute substantially to total leaf hydraulic resistance (Sack & Holbrook, 2006). Although outside-xylem pathways have recently been shown to be the main driver of leaf hydraulic vulnerability under mild and moderate dehydration (Bouche *et al.*, 2016; Trifilo *et al.*, 2016), under severe drought, xylem embolism could induce unrecoverable damage (Knipfer *et al.*, 2015b).

Little is known of the determinants of leaf xylem hydraulic decline. By contrast, numerous studies have investigated the anatomical drivers of decline in stem xylem hydraulic decline during dehydration, and have shown that species with larger and fewer xylem conduits tend to be more vulnerable to drought-induced embolism (Hargrave *et al.*, 1994; Ewers *et al.*, 2007; Cai

& Tyree, 2010; Knipfer *et al.*, 2015a). Additionally, thinner and more porous bordered pit membranes also increase vulnerability to drought-induced embolism in stems (Choat *et al.*, 2008; Li *et al.*, 2016). Both freeze- and drought-induced embolism often initiate in larger xylem conduits near the pith (Cochard & Tyree, 1990; Brodersen *et al.*, 2013). Collapse of leaf vein xylem conduits has been reported in some (Cochard *et al.*, 2004a) but not all gymnosperms (Brodrribb & Holbrook, 2005; Zhang *et al.*, 2014), but has yet to be observed in angiosperms.

According to the hydraulic vulnerability segmentation hypothesis (Tyree & Ewers, 1991), the most distal parts of the xylem pathways should be more vulnerable to hydraulic failure than basal portions. This would allow distal portions to buffer more basal parts from cavitation events, as these supply water to the entire lamina and are therefore less expendable. This hypothesis has been supported by the finding that leaves are more vulnerable to hydraulic decline than stems (Bucci *et al.*, 2012; Pivovaroff *et al.*, 2014). If this hypothesis applies within leaves, the minor veins should be more vulnerable to embolism than the petiole and lower-order veins. Greater susceptibility of higher-order veins would also be consistent with these experiencing the strongest tensions in the plant xylem system. The relative vulnerability of leaf vein orders to embolism formation will influence their contribution to the leaf xylem hydraulic decline. Models and recent imaging techniques have suggested that embolism in the midrib would have a stronger impact on hydraulic conductance than in the smaller diameter minor veins, given the high density of minor veins (McKown *et al.*, 2010; Brodrribb *et al.*, 2016a).

Recent techniques such as optical and neutron imaging permit visualization of spatial and temporal embolism patterns in the entire leaf (Defraeye *et al.*, 2014; Brodrribb *et al.*, 2016b). Based on optical visualization of embolism in leaf veins, a recent study argued that across five broadleaved species, embolism apparently initiated in larger diameter veins, and hypothesized that larger veins contained larger-diameter and thus more vulnerable

conduits than smaller veins (Brodrribb *et al.*, 2016b). However, despite the many advantages of the optical method (cheap, non-destructive, embolism can be visualized throughout the entire leaf in real time), it reveals embolism events within veins while focusing on the projected (paradermal) leaf image and does not allow direct imaging within the vein xylem. Thus, it is not clear whether this method would reveal all embolism events in all veins. In major veins and petioles, the vascular tissue is often composed of hundreds or thousands of conduits embedded deeply within the surrounding tissue and their embolism might not be all visible when observing the leaf optically from above, or even in a paradermal section, but require a cross-sectional view (Fig. 1). Nondestructive, 3D, *in vivo* X-ray microtomography (microCT) imaging allows complete visualization of an entire section of the leaf inside and out, including all veins (from the midrib to the minor veins) at high resolution and therefore provides a valuable complementation to 2D approaches as quantification of individual embolized conduits or the total fraction of functional conduits is needed to relate observed vein embolism events to xylem hydraulic decline (Scoffoni & Jansen, 2016).

By combining hydraulic experiments with microCT and light microscopy imaging of leaf petioles and veins, we addressed three questions: (1) At which water potentials do embolisms become common in specific leaf vein orders? (2) How do leaf petiole and vein xylem conduit diameter in leaves influence vulnerability to drought-induced embolism? (3) How does embolism spread among conduits and vein orders?

Materials and Methods

Plant material

Measurements were conducted from November 2013 to November 2014 on eight species diverse in phylogeny, origin, drought tolerance and life form, growing in and around the campus of the

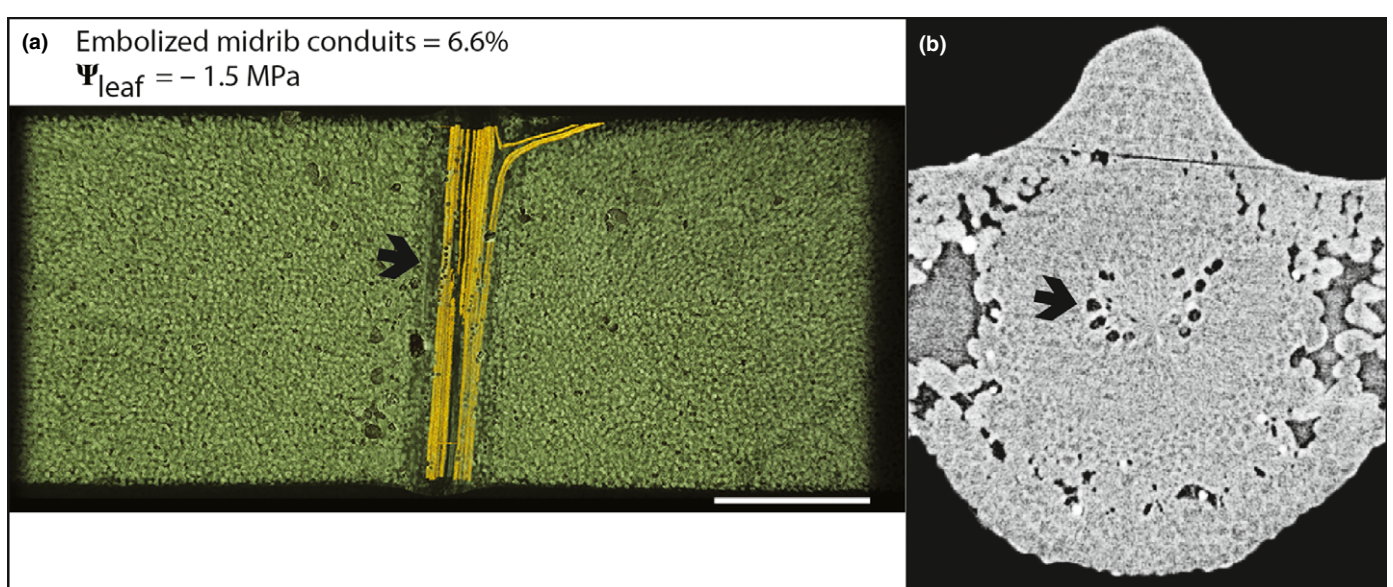


Fig. 1 Paradermal view (a) and cross-sectional view (b) of *Hedera canariensis* micro-tomography scans at mild water potential. The largest veins in the images are leaf midribs. Embolized conduits appear in yellow in (a), and black (b). Black arrows indicate examples of embolized conduits.

University of California, Los Angeles, and Will Rogers State Park (USA). Mature and sun exposed shoots were collected from three to five individuals per species.

Constructing leaf xylem vulnerability curves

In this study, new data from light microscopy and high resolution X-ray micro-computed tomography (microCT) were combined with previously obtained data on leaf xylem hydraulic vulnerability for the same individual plants of eight species (Scoffoni & Sack, 2015; C. Scoffoni *et al.*, unpublished). A variation of the vacuum pump method was used to perform the measurements, as described by Scoffoni & Sack (2015; see Supporting Information Methods S1). Briefly, shoots were dehydrated on the bench to a range of water potentials, then bagged and equilibrated. Two leaves were measured for initial xylem water potential. In the third leaf, minor veins (fourth-order and higher) were cut between c. 95% of tertiary veins throughout the leaf. Using a fresh scalpel, small cuts were made between each tertiary loop, avoiding all major veins. The leaf was then connected underwater by its petiole to a water source (degassed ultra-pure water) on a balance, and placed in a chamber connected to a vacuum pump (0.002 MPa; J4605 Marsh/Bellofram; Marshall Instruments Inc., Anaheim, CA, USA). Five vacuum strengths were applied, from 0.06 to 0.02 MPa. The flow rate of water through the leaf xylem was recorded for every vacuum strength by the change in mass of water on the balance over 30 s. Once the flow stabilized, the flow rate and leaf temperature were recorded. Leaf xylem hydraulic conductance (K_x) was calculated as the slope of flow rate vs vacuum pressure, divided by leaf area and corrected to 25°C to adjust for the effect of temperature on the viscosity of water (Weast, 1974; Yang & Tyree, 1993; Sack *et al.*, 2002). Leaf xylem vulnerability curves were plotted as K_x values against the average of the two Ψ_x values determined at the start of the experiment.

X-ray microtomography

We applied microCT with high-energy X-rays at the synchrotron at the Advanced Light Source (ALS) in Berkeley, California (Beamline 8.3.2) to leaves at different water potentials and imaged the embolism in veins and petioles in December 2014 and April 2015 (see Methods S1). We obtained stacks of images by scanning the center of the leaves (including the midrib), and petiole for four of our study species that exhibited a wide range of drought tolerance, *Comarostaphylis diversifolia*, *Hedera canariensis*, *Lantana camara* and *Magnolia grandiflora*. We attached a small piece of copper wire to the center of either the leaf midrib or petiole using Kapton tape (DuPont, Wilmington, DE, USA), to help center the sample for scanning. To minimize sample movement during the scan, the leaf was enclosed between two half cylinders of styrofoam, and placed in a 9-cm-diameter Plexiglass cylinder, which was then attached to a custom-built aluminum sample holder mounted on an air-bearing stage. To ensure minimal evaporation during the measurement, we placed wet paper towels above the shoot in the plexiglass cylinder. Scans

were made of the midribs and petioles at 18–24 keV in the synchrotron X-ray beam while being rotated 180° with the instrument collecting 1024 projection images in continuous tomography mode. Scans took 8–12 min to complete depending on the scan area selected, and the full 3D internal structure of the leaf midrib and surrounding lamina, and petiole were obtained. Seven to twelve scans of the petiole and midrib (including surrounding mesophyll and higher vein orders) were made per species spanning the range of leaf water potentials obtained in the K_x vulnerability curves (already described).

We quantified conduit embolism in the midrib, higher order veins and petiole for three randomly selected images along the main axis of each imaged leaf (IMAGEJ v.1.46r; National Institutes of Health, USA). Three-dimensional volume renderings of our scans were made using AVIZO 8.1.1 software (VSG Inc., Burlington, MA, USA), and used to determine the number of embolized conduits in the petiole and all vein orders, identifying vein orders by following the branching pattern from the secondary veins. We also determined the connectivity between embolized conduits within and among different vein orders.

We calculated the percentage of embolized conduits in the midrib (%EMC) at given leaf water potentials. We could not resolve nonembolized conduits in the scanned leaves; attempts to re-scan leaves after drying such that all embolized conduits could be counted were not successful because the shrinkage of leaf tissues in the midrib and petiole led to the inability to resolve them in the image. Thus, we estimated the total number of midrib conduits in the scanned leaves by using measurements taken from cross-sections of three leaves of the same plants of each species visualized by light microscopy (Fig. 2). Given that the number of midrib xylem conduits scales with the midrib vascular cross-sectional area for well hydrated leaves of given species (Coomes *et al.*, 2008; Taneda & Terashima, 2012), we counted the total number of xylem conduits in the midrib cross-sections for hydrated leaves under light microscopy and normalized conduit number by midrib vascular area. These values were averaged for each species to estimate conduit number per vascular area for hydrated leaves (CNA_{hydr}). To calculate the total number of midrib conduits in cross-sections of the scanned dehydrated leaves (CNA_{dehyd}), which showed substantial shrinkage of the midrib vascular area, we plotted midrib vascular area for the dehydrated leaves (A_{dehyd}) against leaf water potential for each species to estimate the proportion of vascular area shrinkage (PVAS) by extrapolating to 0 MPa. The conduit number for each individual scanned leaf was obtained as:

$$CN = CNA_{hydr} \times \frac{A_{dehyd}}{1 - PVAS}. \quad \text{Eqn 1}$$

We counted the number of embolized conduits in each scanned leaf (CN_{emb}) and calculated %EMC as:

$$\%EMC = \frac{CN_{emb}}{CN} \times 100. \quad \text{Eqn 2}$$

For petioles, the number of embolized conduits was calculated in all scans, and normalized by leaf area given that studies have

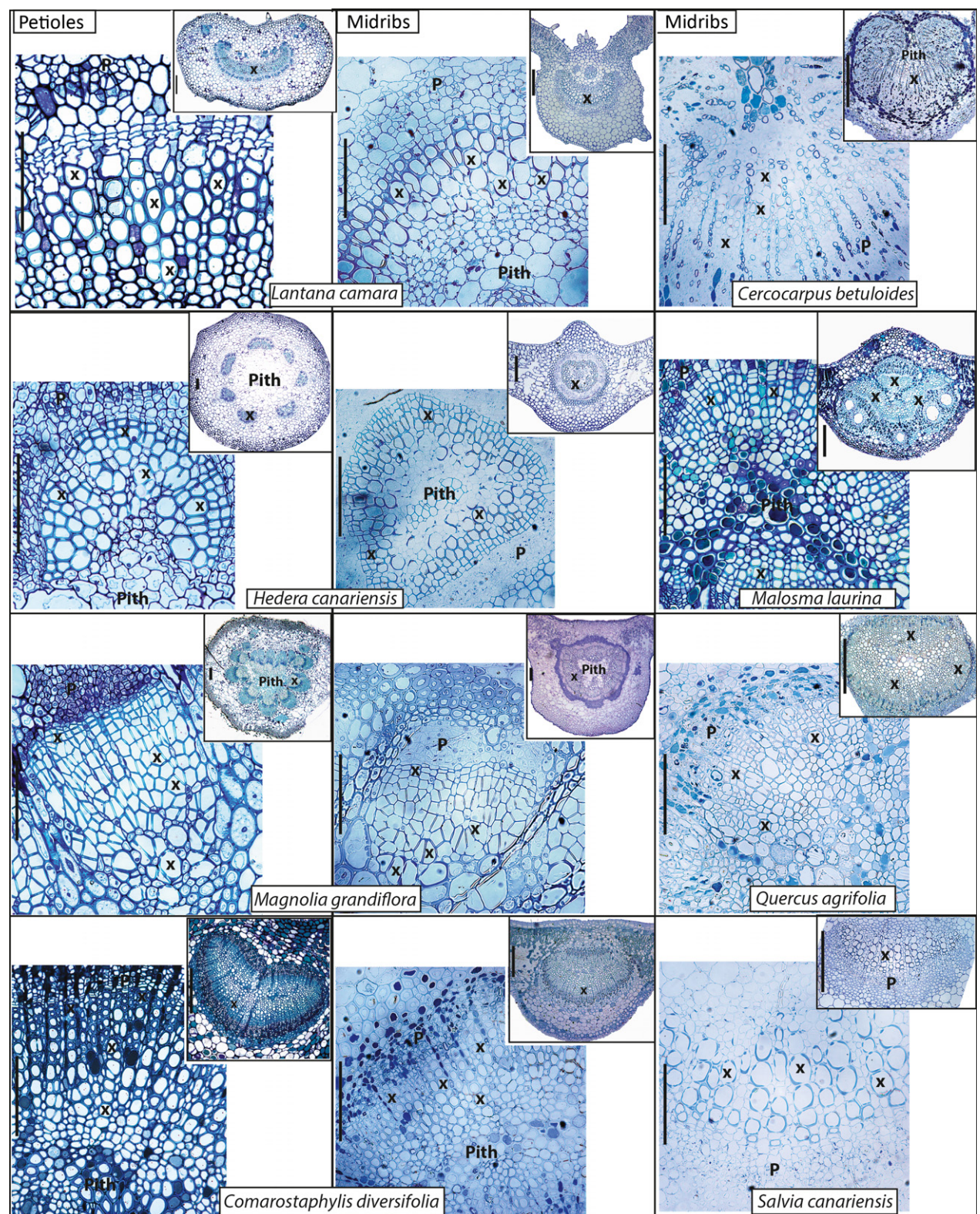


Fig. 2 Petiole cross-sections for the four species used for X-ray micro-computed tomography, and midrib cross-sections for all eight species imaged by light microscopy. Examples of xylem conduits are marked by an 'X' in each image. P, Phloem. Bars, 100 µm (250 µm in the insets).

shown a tight scaling of petiole xylem area and leaf size for given species (Salisbury, 1913; Taneda & Terashima, 2012). Light-microscope images of three petiole cross-sections per species were

obtained to count the total number of xylem conduits normalized by leaf area (Fig. 2). The percentage of embolized petiole conduits (%EPC) was obtained for each scan by dividing the number

of embolized conduits per leaf area by the total number of conduits per leaf area.

Scaling up the influence of embolized xylem conduits to the whole leaf xylem system

Our application of microCT had resolution high enough to visualize all of the embolized conduits, but not enough to measure their exact dimensions which directly influences leaf xylem hydraulic conductance (K_x). We used a spatially explicit model of a leaf vascular network (K_{LEAF} ; Cochard *et al.*, 2004b; McKown *et al.*, 2010; Scoffoni *et al.*, 2011, 2014) to simulate the impact of the observed embolism on hydraulic conductance under different scenarios for a relationship of conduit embolism with size.

K_{LEAF} calculates xylem and total leaf hydraulic conductance given inputs of leaf size, vein densities and cross-sectional conductivities for each vein order and an input value for outside-xylem conductance. For parameterizing K_{LEAF} , cross-sectional theoretical conductivities of midrib and minor veins for each species were calculated from Eqn 3 below, using conduit dimensions obtained from light-microscopy (Figs 2, S1, S2; Table S1). Because we did not have cross-sectional images of second- and third-order veins, we obtained cross-sectional theoretical conductivities for these two vein orders using a ‘two-point allometry’ method. Consistent tapering of conduit diameters and decline of conduit numbers across vein orders results in a tight correlation between conduit size and vein orders, which translates into a tight negative correlation between cross-sectional conductivities (K_t) and vein order number for a given species (Cochard *et al.*, 2004b; Coomes *et al.*, 2008; Sack & Scoffoni, 2013). The correlation is so tight that fitting a power law to two points (K_t of midrib and K_t of fifth-order vein) allows an estimation of K_t for second- and third-order veins. When testing this approach using data available for *Laurus nobilis* (Cochard *et al.*, 2004b), the K_t values estimated in this way for second- and third-order veins were 90% and 100%, respectively, of true measured values (data not shown). Finally, for each species, we input into K_{LEAF} the mean values for leaf lengths, widths and second-order vein numbers obtained for the same individual plants of each species from a previous study (Scoffoni *et al.*, 2011). Model inputs for each species and treatment can be found in Table S1. Simulations assumed an elliptical leaf without tapering along the length of midrib and second-order veins and with connectivity among all veins in contact (i.e. nonsectorial system). Areole widths and lengths were modified for each species to yield leaf areas similar to observed averages for each species (Table S1).

We applied the model for simulations of the four species used for microCT at five leaf water potentials (Ψ_{leaf}) spanning each species’ observed ranges in the experiments. For each of these Ψ_{leaf} we had data for the %embolized conduits for each vein order observed from the microCT images (using direct counts for midrib, and estimated values based on Table 1; input values can be found in Table S1). Previous studies of stem embolism have shown that larger conduits tend to embolize first (Brodersen *et al.*, 2013; Knipfer *et al.*, 2015a). To bind the estimated effect on K_x according to the potential relationships of midrib

embolism to conduit size, we ran the model estimating K_x according to three scenarios: (1) midrib embolism reduced midrib conductivity independently of conduit size, or alternatively, embolized conduits occurred in (2) the largest or (3) the smallest midrib conduits. In scenario 1, K_t for each water potential interval was reduced by the percent embolized conduits recorded for that water potential. In scenarios 2 and 3, we first ordered all the conduits measured for each individual plant in light microscopy from largest to smallest. We then assumed that the number of embolized conduits obtained from microCT were the largest (or smallest) conduits in our dataset. We thus calculated the total K_t of the largest (or smallest) embolized conduits at each water potential interval, and subtracted that value from the maximum K_t (Table S2). For second- and third-order and minor veins, we calculated K_t for each water potential interval by reducing maximum K_t by the percentage of embolized conduits estimated from Table 1 for each water potential interval (Table S2). This assumes embolized conduits were of similar and average dimensions in those vein orders. The percentage loss of K_x was obtained for each simulation by dividing the K_x of the given simulation by that obtained at $\Psi_{\text{leaf}} = 0 \text{ MPa}$.

Modeling the potential influence of minor vein conduit collapse on K_x decline

Although xylem conduit collapse in angiosperms has never been observed, we investigated the consequences of such collapse occurring in minor veins, given that leaves strongly shrink in area and thickness during dehydration (Scoffoni *et al.*, 2014). Because we imaged at a 3.2- μm resolution, we were unable to observe xylem conduit collapse with microCT due to low localized contrast with surrounding tissue. Therefore, we modeled the potential hydraulic impact of conduit collapse on K_x using K_{LEAF} . We assumed that no collapse occurs before turgor loss point as for pine species in which such collapse was observed (Cochard *et al.*, 2004a), and also given that our study species show only slight shrinkage above turgor loss point (Scoffoni *et al.*, 2014). We considered two scenarios: (1) collapse of minor vein conduits would induce 30% decline in vein conductivity at turgor loss point and $\leq 70\%$ at extreme dehydration levels, as was observed in pine needles (Cochard *et al.*, 2004a), and (2) collapse is extreme, reducing the conductivity of minor and third-order veins by 90% at turgor loss point and $\leq 99\%$ at extreme dehydration levels. The model was parameterized as for scaling up the influence of embolism on K_x as described in the section above, assuming that the largest conduits in the midrib embolized first. Model parameters can be found in Table S3.

Light microscopy of petioles, midribs and minor veins

We obtained petiole cross-sections for the four species used in microCT. Briefly, from each petiole center, a 0.5-cm section was cut and embedded gradually in low-viscosity acrylic resin (L. R. White; London Resin Co., London, UK) in ethanol, and under vacuum over the course of a week. The samples were then dried

Table 1 Observations of embolized conduits in X-ray micro-computed tomography (microCT) analyses in the different leaf vein orders of the four studied species during leaf dehydration to low leaf water potentials, and the range of leaf water potentials at which embolism was first observed

Species	Petiole	Midrib	Secondary veins	Third-order veins	Fourth-order veins	Fifth-order veins	FEVs
<i>Lantana camara</i>	-0.1 to -1.0 MPa (few), <-1 MPa (common)	-0.1 (few) to -1.4 MPa (common)	-0.95 MPa to -1.4 MPa (few)	None	None	None	None
	-0.1 to -3.4 MPa (few), <-3.5 MPa (common)	-0.2 to -3.4 MPa (few), -4 MPa (common)	-0.33 MPa (few), <-1.53 MPa (common)	-1.53 to -4.0 MPa (common)	-4 MPa (few)	-4 MPa (few)	None
<i>Hedera canariensis</i>	-0.1 to -3.4 MPa (few), <-3.5 MPa (common)	-0.08 to -1.7 MPa (few), <-3.5 MPa (common)	-0.08 to -1.7 MPa (few), <-3.5 (common)	-1.6 to -3.6 MPa (few), -7.6 MPa (common)	-7.6 MPa (few)	-7.6 MPa (few)	None
	-0.1 to -1.0 MPa (few), <-3.5 MPa (common)	Few across range	-0.01 to -5.9 MPa (few), <-5.9 MPa (common)	-3.5 to -5.9 MPa (few), <-5.9 (common)	-5.9 to -7.2 MPa (few)	-5.9 to -7.2 MPa (few)	None
<i>Magnolia grandiflora</i>							
<i>Comarostaphylis diversifolia</i>							

FEVs, free ending veins.

n = 9–12 leaves observed per species across the range of leaf water potentials. ‘Few’ signifies <15% of conduits were embolized in petioles and major veins (midrib, secondary and tertiary veins), and <5 minor veins embolized within the leaf section scanned.

at 55°C overnight, and sectioned using glass knives (cut using a LKB 7800 KnifeMaker; LKB Produkter, Bromma, Sweden) at 1-μm thickness in a rotary microtome (Leica Ultracut E, Reichert-Jung, CA, USA). Sections were stained in 0.01% toluidine blue in 1% sodium borate and imaged using a ×5, 10, 20 and 40 objective using a light microscope (Leica Lietz DMRB; Leica Microsystems, Wetzlar, Germany) with camera utilizing SPOT advanced imaging software (SPOT Imaging Solutions; Diagnostic Instruments Inc., Sterling Heights, MI, USA) for a total image magnification of ×287 to ×2300.

For measurements of midrib and minor vein cross-sectional anatomy, we prepared cross-sections for *Malosma laurina* using the same method described above for petioles, and used images published previously for the same individuals of the seven remaining species (John *et al.*, 2013). Using IMAGEJ (National Institutes of Health), we measured the vascular bundle area in the midrib, the xylem conduit diameters in the midrib and petiole, and counted the total number of xylem conduits in each section. The total number of conduits and maximum conduit areas (calculated from the major and minor axes of conduits, and assuming that conduits are ellipses) were averaged across the midribs of the three sections. Additionally, we determined the theoretical conductivity of xylem conduits in the midrib and minor veins of each leaf using Poiseuille’s equation modified for ellipses (Lewis & Boose, 1995; Cochard *et al.*, 2004b):

$$K_t = \sum \frac{\pi a^3 b^3}{64 \eta v_w (a^2 + b^2)}, \quad \text{Eqn 3}$$

(*a* and *b*, major and minor (respectively) axes of xylem conduit; η , dynamic viscosity of water at 25°C; v_w , molar volume of water).

Measurement of turgor loss point

Leaf turgor loss point for all species was obtained from pressure–volume curves of previously published studies that were based on the same individual plants of the study species (Scoffoni *et al.*, 2012, 2014; C. Scoffoni *et al.*, unpublished).

Statistics

In order to identify the best equations to describe vulnerability curves, we selected the maximum likelihood function for each species using the OPTIM function in R 3.1.0 (<http://www.r-project.org>; Burnham & Anderson, 2004; Scoffoni *et al.*, 2012; the scripts are available on request), testing five functions (see Methods S1).

All trait relationships were analyzed using standard major axes (SMA; using SMATR; Warton *et al.*, 2006) such that traits were considered as independent variables with similar measurement error. When the relationship was apparently linear, SMA was performed on untransformed data, and when the relationship was nonlinear, on log-transformed data to model a power law relationship (Xiao *et al.*, 2011).

Results

Our experiments indicated that embolisms in the midrib and petiole, not minor veins, play an important role in leaf xylem hydraulic decline during dehydration, and that xylem conduit dimensions determine both the pattern of embolism and of hydraulic decline.

X-ray microtomography of petiole and leaf veins for four species revealed that xylem embolism occurred predominantly in the petiole and midrib conduits (Figs 3–8; Table 1). Embolism from the midribs rarely extended to secondary or tertiary veins even under severe stress for each species (Figs 5–8; Table 1). By contrast, we found negligible embolism in minor veins, and this occurred only in extremely dehydrated leaves (Table 1). Further,

embolisms were rare overall across the range of water potentials, with 50% of embolized conduits occurring only at very negative water potentials, or never as in the case of *Comarostaphylis diversifolia*. Finally, embolized conduits in the midrib and petiole were often connected with one another, although there were a few cases of isolated embolized conduits in the petioles of all four species, secondary veins of *L. camara*, and in tertiary and minor veins of *C. diversifolia*, *H. canariensis* and *M. grandiflora* (Fig. 9).

Model simulations of the influence of embolism on the decline of whole leaf xylem hydraulic conductance revealed a general importance of midrib conduit size. Among three alternative simulations that assumed embolism (1) caused decline of vein conductivity independently of conduit size, or that embolism occurred in (2) the largest, or (3) the smallest conduits,

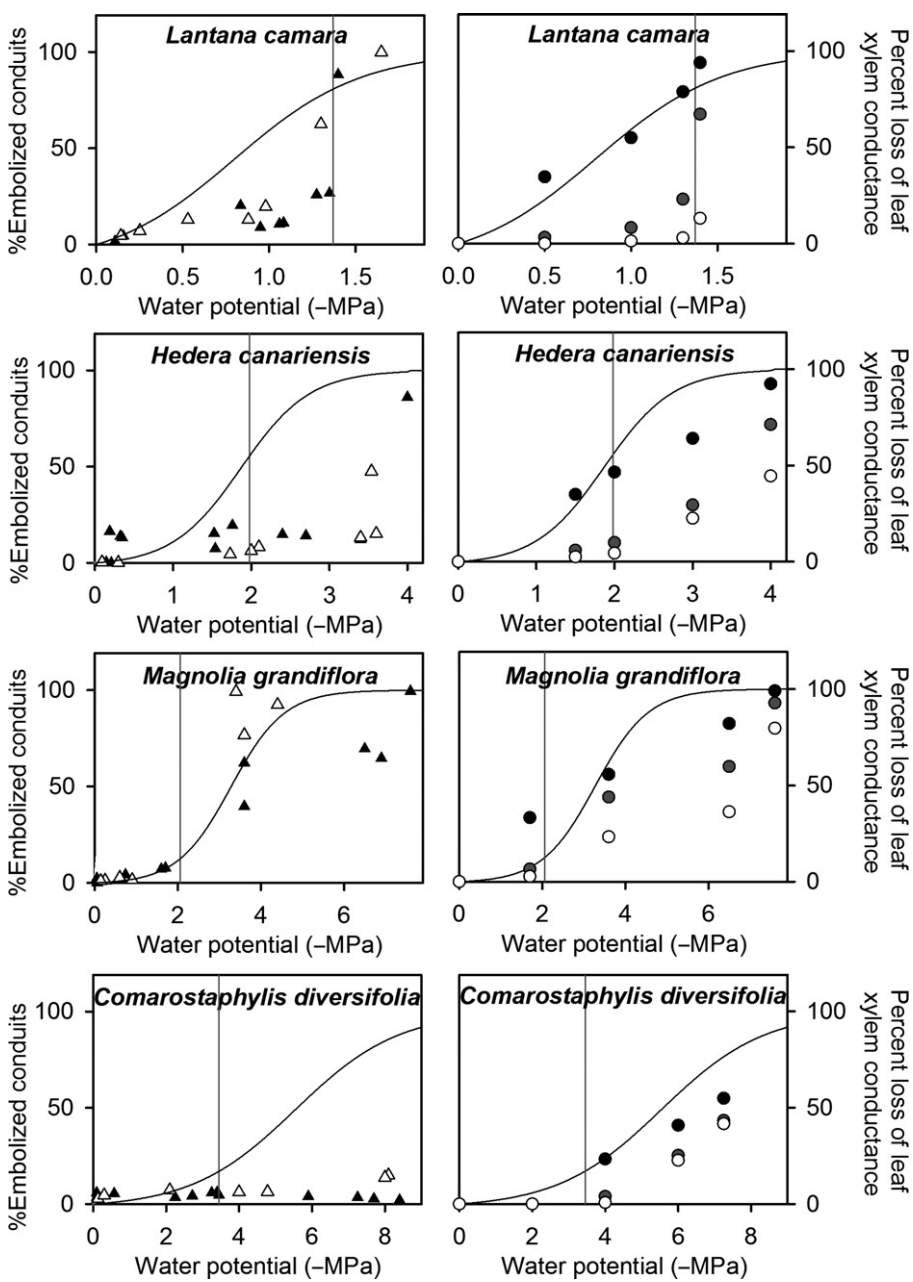


Fig. 3 Increase in the percentage of embolized conduits in the leaf petiole (white) and midrib (black) with dehydration for four species diverse in phylogeny and drought tolerance. Panels on the right are results from model simulations using K_{LEAF}. Simulations were run to estimate the leaf xylem hydraulic conductance K_x in the scenario (1) all conduits are of the same size (gray); (2) the largest conduits embolize (black points); and (3) the smallest conduits embolize (white). The solid line in both left and right panels represents the maximum likelihood function that best fitted the measured percent loss of xylem hydraulic conductance. The gray vertical line represents the leaf bulk turgor loss point.

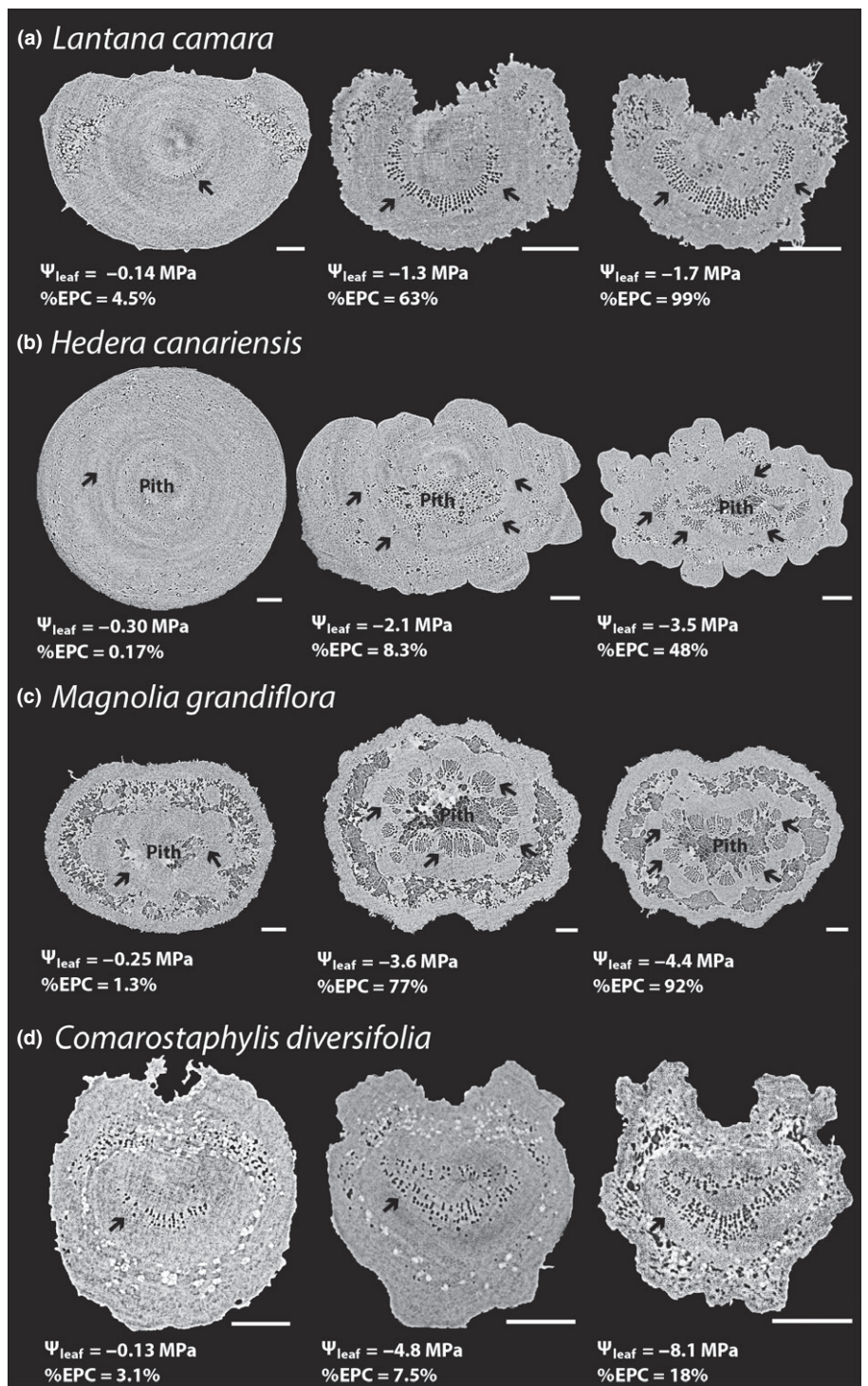


Fig. 4 *In vivo* imaging of leaf petioles of four species diverse in phylogeny and drought tolerance, subjected to progressive dehydration. (a–d) X-ray micro-computed tomography scans of petioles at mild, medium and high levels of dehydration. Black arrows point to conduits that are air-filled (i.e. embolized). In *Comarostaphylis diversifolia*, embolized conduits of both protoxylem (hydraulically nonfunctional) and metaxylem are shown by black arrows. Ψ_{leaf} , leaf water potential; %EPC, percentage of embolized petiole xylem conduits. Bars, 250 µm.

simulation 2 produced the best match between the predicted and observed percentage loss of leaf xylem hydraulic conductivity (K_x PLC); simulations 1 and 3 generally underestimated the observed PLC (Fig. 3). PLC values predicted under the largest conduit scenario were tightly correlated with measured PLC across all water potentials tested (Fig. 10), with slopes close to unity in all species when regressions were forced through the origin, indicating little bias (Fig. 10). By contrast, predicted and observed PLC were

uncorrelated in the other two scenarios (assuming either embolism occurred evenly across conduit sizes, or that smallest conduits embolized first) for *L. camara* and *H. canariensis* ($P=0.06–0.20$), and predicted PLC was correlated with but consistently lower than observed PLC in *M. grandiflora* and *C. diversifolia* ($P=0.005–0.047$; slopes of 0.79 and 0.57 for *M. grandiflora* and 0.50 and 0.46 for *C. diversifolia* in the mean and small conduit scenarios, respectively).

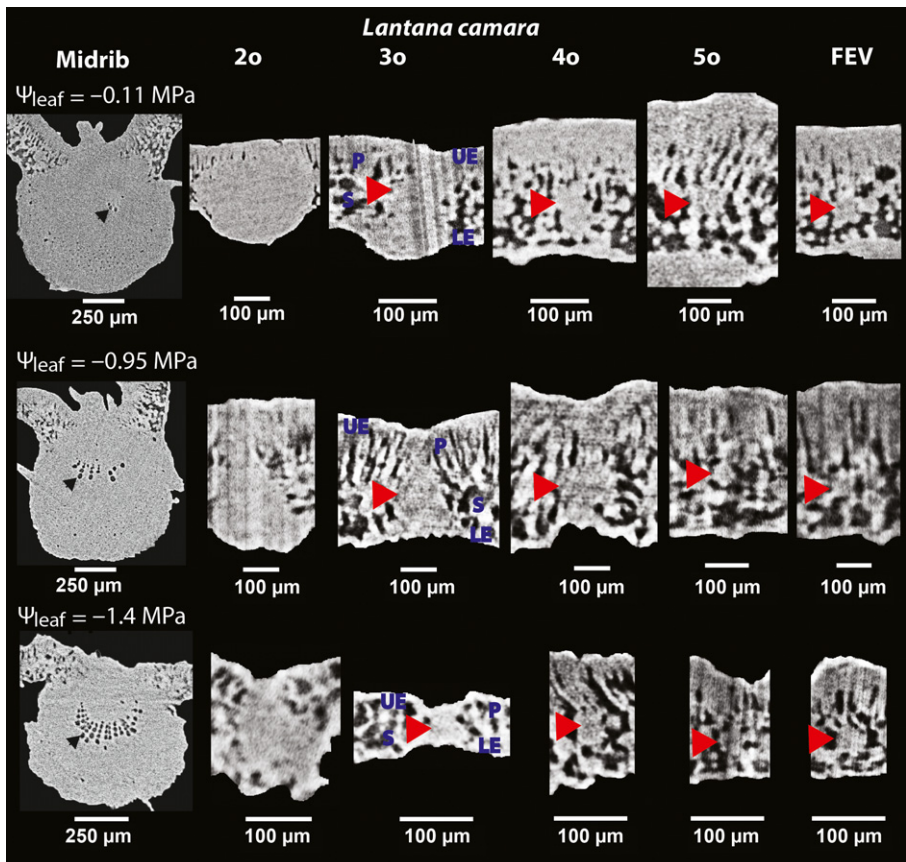


Fig. 5 *In vivo* imaging of leaf midribs, tertiary and minor veins of four species diverse in phylogeny and drought tolerance, subjected to progressive dehydration. X-ray micro-computed tomography scans of midribs, secondary, third-, fourth-, fifth- and sixth-order (= free ending veins; FEV) veins at mild, medium and high levels of dehydration are shown for *Lantana camara*. Third-order and minor vein orders were determined from the 3D reconstruction of the leaf scan. Black arrows point to embolized conduits. Note that third-order and minor veins are never embolized. Ψ_{leaf} , leaf water potential; UE, upper epidermis; P, palisade mesophyll; S, spongy mesophyll; LE, lower epidermis. Red arrows point to vascular bundles in tertiary and minor veins.

Simulations showed very little impact of any potential xylem conduit collapse of minor and third-order veins on the decline of leaf xylem hydraulic conductance (K_x) (Fig. 11). Simulating 30–70% decline of minor vein conductivity due to collapse from turgor loss point to extreme dehydration levels increased the percentage loss of whole leaf xylem conductance only by 0.15–4.3% across species (Fig. 11). Even when simulating an extreme influence of minor and third-order vein collapse on K_x decline – that is, a 90–99% decline of conductivity from turgor loss point to extreme dehydration levels – only 0.72–14% increase in the percentage loss of leaf xylem conductance was observed across water potentials and species (Fig. 11).

We found a significant relationship of leaf xylem vulnerability to midrib and petiole conduit size across eight diverse species. Our results showed a significant correlation between the water potential at which K_x declined by 50% ($P_{50}K_x$) or 88% ($P_{88}K_x$) and the average size and number of midrib xylem conduits (Fig. 12a,b, $r^2=0.72$ and 0.54 for the correlation of $P_{88}K_x$ with conduit size and number, respectively; $P<0.05$). Similarly, petiole and midrib average conduit size correlated with the water potential at which 50% of embolized conduits was observed with the microCT ($r^2=0.82$ –0.88; $P<0.05$). By contrast, neither $P_{50}K_x$ nor $P_{88}K_x$ correlated with minor vein conduit size or number ($P=0.34$ –0.83). We measured petiole conduit diameters and numbers for four species and found strong overlap with midrib conduits, although petioles tended to have slightly larger xylem conduits (mean \pm SE: $86.5 \pm 11.6 \mu\text{m}^2$ for petioles vs

$69.0 \pm 8.73 \mu\text{m}^2$ for midribs; $P=0.038$ using a nested-ANOVA with petiole vs midrib nested within species; Fig. 2) and petioles and midribs were statistically similar in conduit numbers (1124 ± 192 vs 1055 ± 234 ; $P=0.696$; Fig. 2). The similar vulnerabilities between midrib and petiole observed under microCT (see Results above) was thus also consistent with a general association of conduit size with vulnerability to embolism (Fig. 12).

Finally, we investigated the scaling of conduit anatomy and vein sizes across our species set. We found no significant relationships between midrib diameter and mean midrib conduit area ($P=0.29$) or midrib conduit number ($P=0.40$) (Fig. S3). Further, we found no significant correlation across the eight species between midrib or petiole diameter and either $P_{50}K_x$ or $P_{88}K_x$ ($P=0.21$ –0.36).

Discussion

Our results provide a critical new understanding of leaf xylem hydraulic decline with dehydration, pointing to the strong role of xylem conduit anatomy and vein hierarchy in xylem safety. In particular, midrib and petiole conduit anatomy, not minor veins, were found to determine leaf xylem vulnerability. Three-dimensional, X-ray microtomography (microCT) imaging revealed embolism formation in petiole and midribs during strong leaf dehydration. However, minor veins were extremely resistant to embolism induction. In *Lantana camara*, embolism in the minor veins was not observed within the range of leaf water

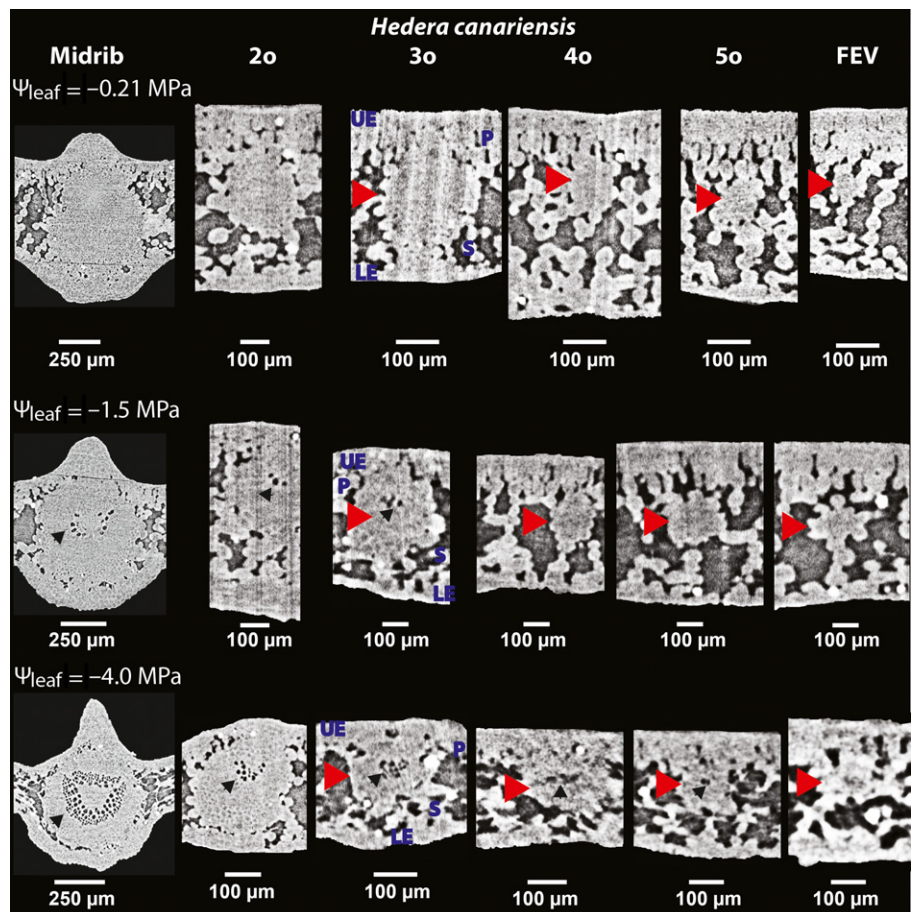


Fig. 6 *In vivo* imaging of leaf midribs, tertiary and minor veins of four species diverse in phylogeny and drought tolerance, subjected to progressive dehydration. X-ray micro-computed tomography scans of midribs, secondary, third-, fourth-, fifth- and sixth-order (= free ending veins; FEV) veins at mild, medium and high levels of dehydration are shown for *Hedera canariensis*. Third-order and minor vein orders were determined from the 3D reconstruction of the leaf scan. Note that third-order and minor veins are rarely embolized, and only at very high levels of leaf dehydration, and that no conduits in the free ending veins were embolized across the range of water potential investigated (Table 1). Ψ_{leaf} , leaf water potential; UE, upper epidermis; P, palisade mesophyll; S, spongy mesophyll; LE, lower epidermis. Red arrows point to vascular bundles in tertiary and minor veins.

potentials the species would experience even under extreme field drought conditions. In the three remaining species, K_x had already declined by 99% in *Magnolia grandiflora* and *Hedera canariensis*, and by 55% in *Comarostaphylis diversifolia* before any sign of minor vein embolism could be observed. In accordance with our microCT results, we found that xylem vulnerability to hydraulic decline was independent of both minor vein conduit sizes and numbers, but highly correlated with midrib conduit sizes and numbers. Our results from microCT performed on petioles of four species showed that petioles behave similarly to midribs, with similar percentages of embolized conduits at given Ψ_{leaf} , and these embolized conduits would likely have the same hydraulic impact on K_x as they were of similar size.

The effect of conduit anatomy on leaf xylem hydraulic decline

The relationship of leaf xylem vulnerability curve to patterns of embolism in vein xylem revealed by microCT indicates that the sizes of conduits which embolize are important in determining vulnerability both within vein orders of given species, and, equally, across species. We found a strong correspondence of leaf xylem vulnerability curve with the percentage number of embolized conduits in the midrib and petiole in *M. grandiflora*, but not for the other three species in which leaf xylem hydraulic conductance (K_x) declined more steeply with leaf dehydration than the number of embolized conduits *per se* (Fig. 3). However,

our computer simulations showed that this apparent mismatch could be explained by larger conduits embolizing first, which would drive a disproportionate decline in K_x according to Hagen–Poiseuille's Law. This explanation was supported by our finding that the scenario in which the largest conduits embolized first best explained the measured declines in K_x for every species. The remaining mismatch between the decline of simulated K_x based on embolism of conduits and that of measured K_x were consistent with factors not accounted for in the model. Even though K_LEAF is an explicit model of leaves, parameterized with real anatomical data for each species (see the Materials and Methods section and Tables S2, S3), it does not include the petiole. For *H. canariensis*, for example, simulations of embolism using the largest conduits in the midrib yielded values of K_x at high tensions that were slightly lower than those measured in the hydraulics experiments, which could be explained by the fact that this species has a long petiole, which would contribute more to the leaf hydraulic resistance and thus embolism would have a stronger impact on K_x than modeled. Because we lacked data on xylem conduit size distributions within second- and third-order veins, we assumed those to be all of equal size, which could slightly underestimate the percentage loss of conductance values from our simulations. Despite these model limitations, midrib embolism under the scenario where the largest conduits embolize first explained most of the observed decline in K_x . The assumption that larger conduits embolize first is consistent with the

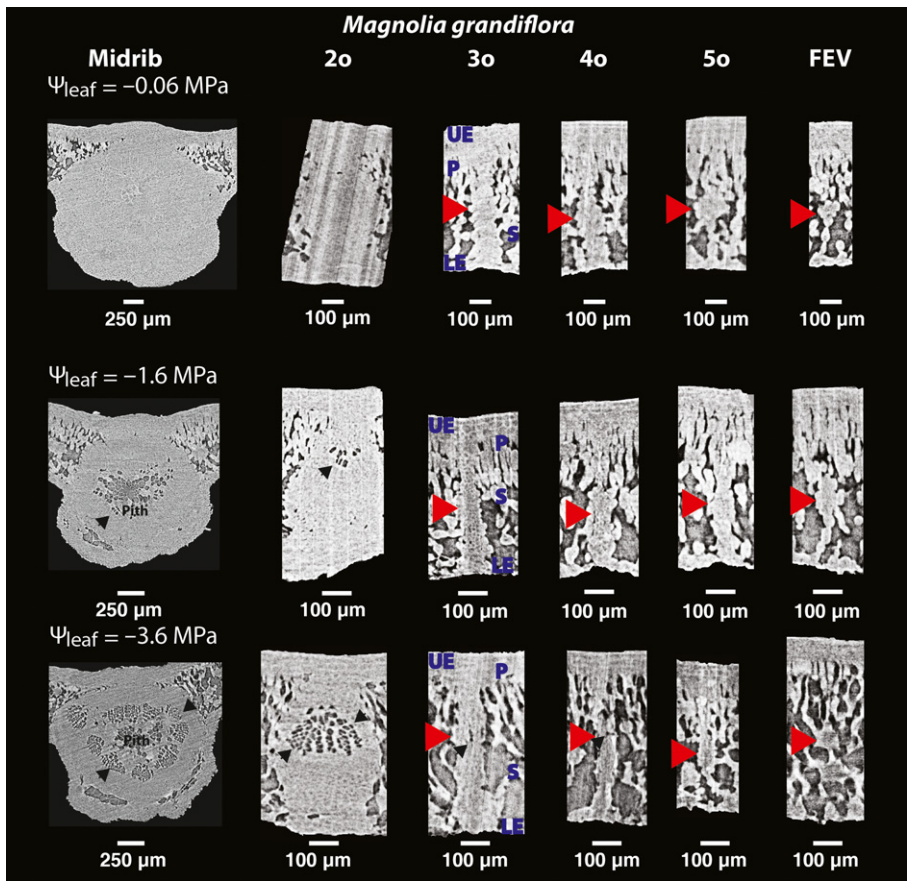


Fig. 7 *In vivo* imaging of leaf midribs, tertiary and minor veins of four species diverse in phylogeny and drought tolerance, subjected to progressive dehydration. X-ray micro-computed tomography scans of midribs, secondary, third-, fourth-, fifth- and sixth-order (= free ending veins; FEV) veins at mild, medium and high levels of dehydration are shown for *Magnolia grandiflora*. Third-order and minor vein orders were determined from the 3D reconstruction of the leaf scan. Note that third-order and minor veins are rarely embolized, and only at very high levels of leaf dehydration, and that no conduits in the free ending veins were embolized across the range of water potential investigated (Table 1). Ψ_{leaf} , leaf water potential; UE, upper epidermis; P, palisade mesophyll; S, spongy mesophyll; LE, lower epidermis. Red arrows point to vascular bundles in tertiary and minor veins.

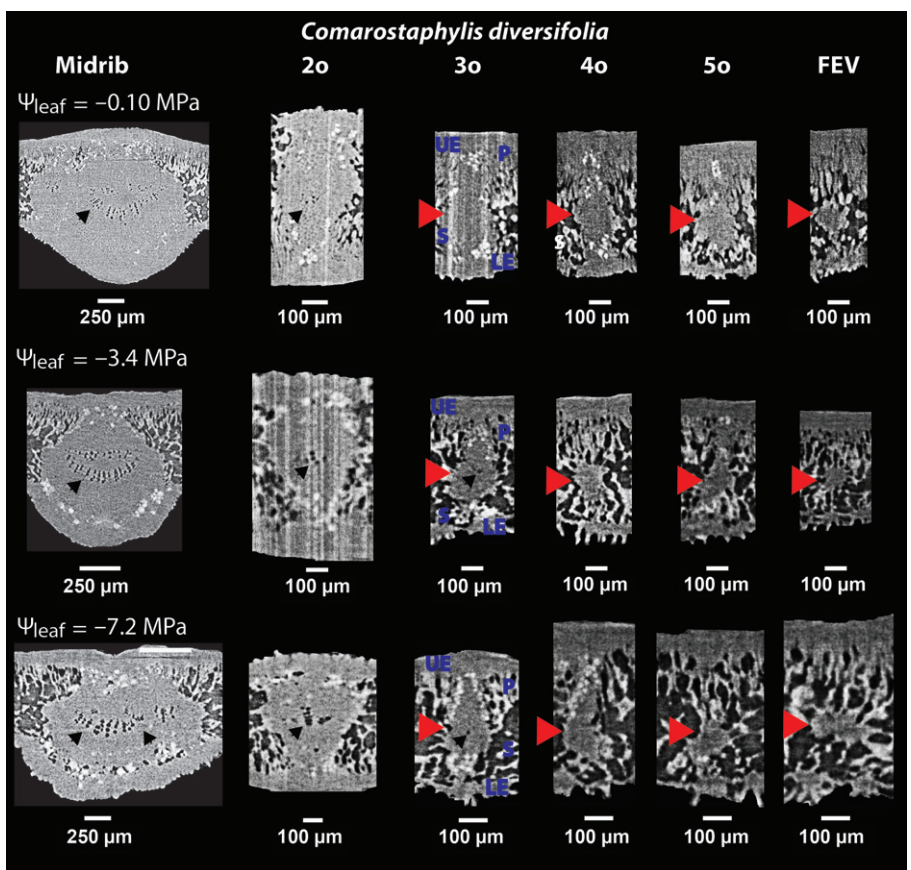


Fig. 8 *In vivo* imaging of leaf midribs, tertiary and minor veins of four species diverse in phylogeny and drought tolerance, subjected to progressive dehydration. X-ray micro-computed tomography scans of midribs, secondary, third-, fourth-, fifth- and sixth-order (= free ending veins; FEV) veins at mild, medium and high levels of dehydration are shown for *Comarostaphylis diversifolia*. Third-order and minor vein orders were determined from the 3D reconstruction of the leaf scan. Black arrows point to embolized conduits. Black arrows in leaf midrib point to embolized conduits that could either be protoxylem (i.e. nonfunctional) and/or metaxylem. Note that third-order and minor veins are rarely embolized, and only at very high levels of leaf dehydration, and that no conduits in the free ending veins were embolized across species and range of water potential investigated (Table 1). Ψ_{leaf} , leaf water potential; UE, upper epidermis; P, palisade mesophyll; S, spongy mesophyll; LE, lower epidermis. Red arrows point to vascular bundles in tertiary and minor veins.

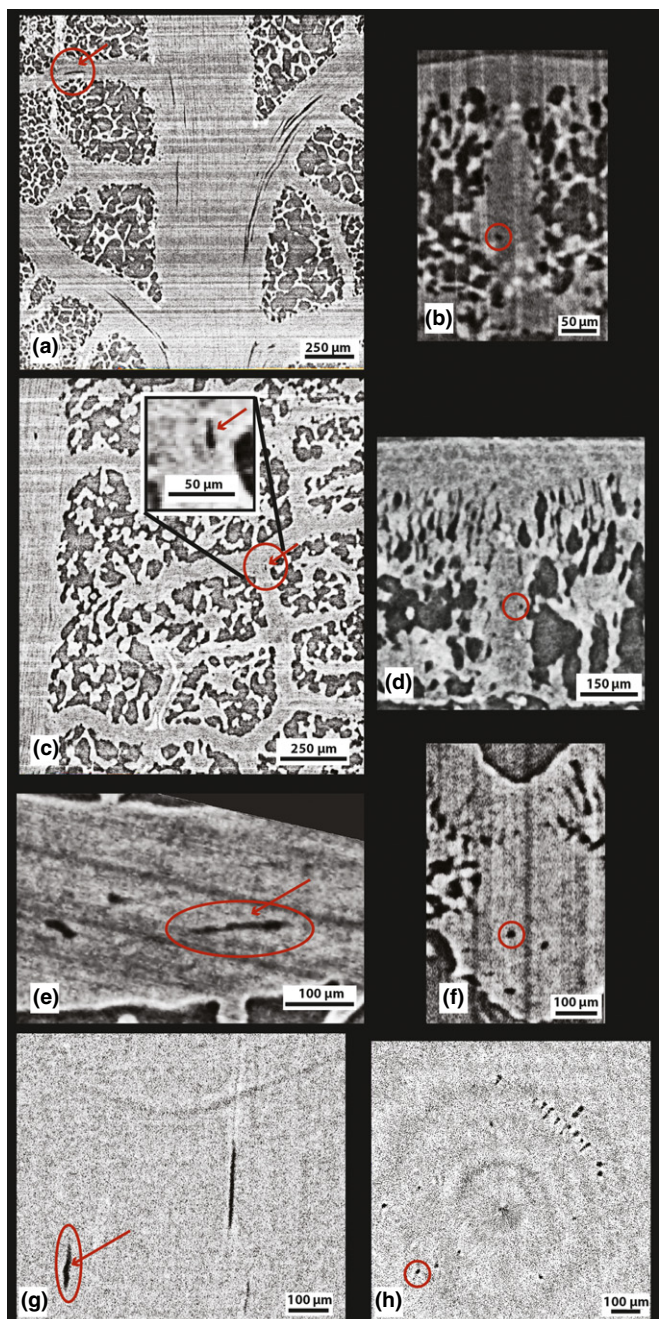


Fig. 9 Isolated embolized conduits in leaf petioles and veins, circled in red. Longitudinal (a) and cross-sectional (b) view through *Comarostaphylis diversifolia* leaf veins at -7.7 MPa, with an isolated embolized conduit in a third-order vein. Longitudinal (c) and cross-sectional (d) view of *Magnolia grandiflora* leaf veins at -3.0 MPa, with an isolated embolized conduit in a fourth-order vein. Longitudinal (e) and cross-sectional (f) view of *Lantana camara* leaf veins at -0.95 MPa, with an isolated embolized conduit in a secondary vein. Largest vein in (a, c, e) is the midrib. Longitudinal (g) and cross-sectional (h) view of *Lantana camara* at -0.14 MPa, with an isolated embolized conduit in the petiole.

observation from microCT imaging that conduits closest to the pith tend to be more susceptible to embolism formation (Figs 2–6), a pattern also seen in stems (Brodersen *et al.*, 2013). Indeed,

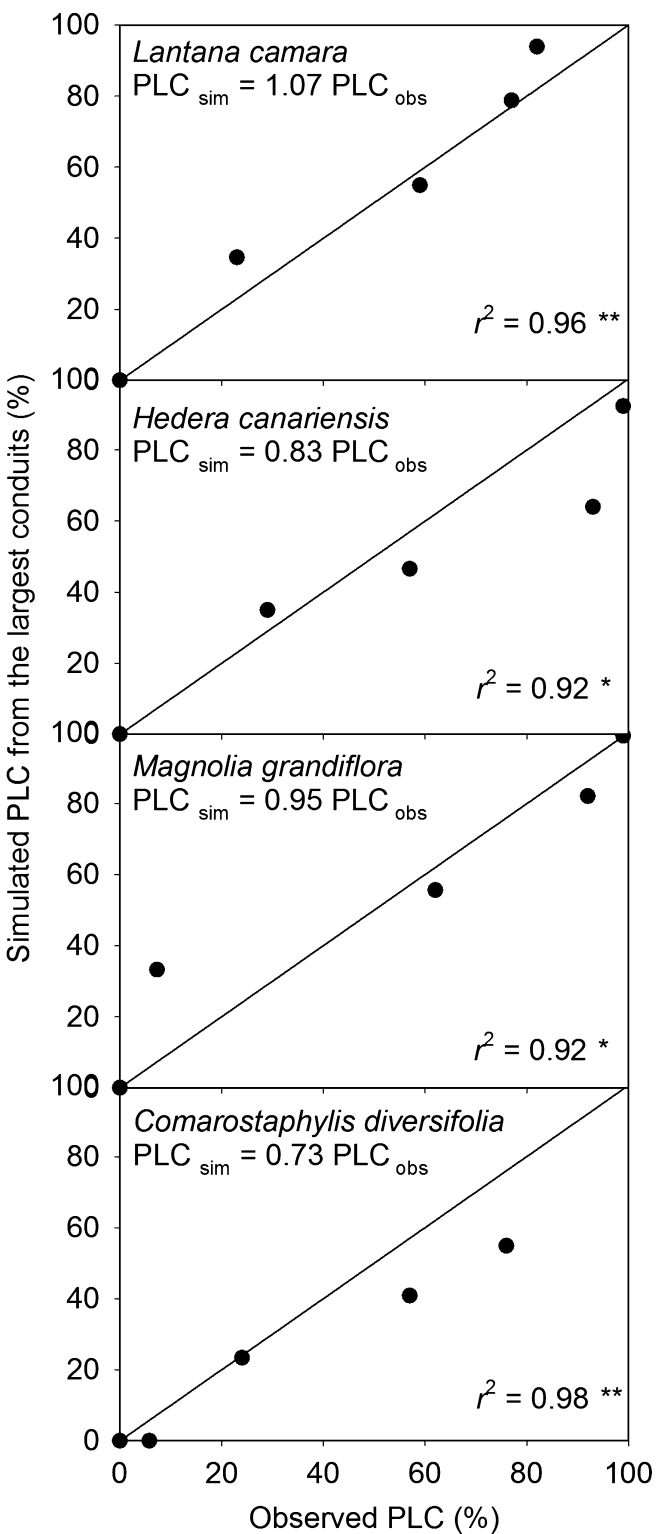


Fig. 10 Tight correspondence of the simulated percentage loss of xylem conductivity (PLC) using X-ray micro-computed tomography (microCT) observation of embolized xylem conduits with the observed leaf xylem PLC across four diverse species. The PLC simulated with K_{LEAF} shown here on the y-axis assumed that the embolized conduits observed with microCT corresponded to the largest conduits in the midrib. *, $P < 0.05$; **, $P < 0.01$.

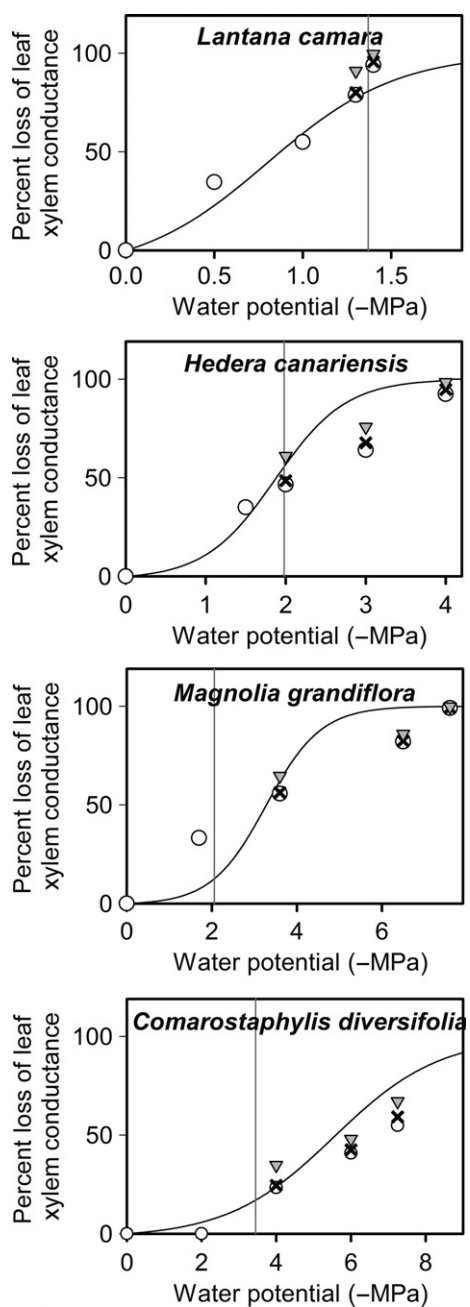


Fig. 11 Results from model simulations using K_{LEAF} to investigate the potential effect of xylem conduit collapse after turgor loss point in minor and third-order veins on the decline of leaf xylem hydraulic conductance. Simulations were run to estimate leaf xylem hydraulic conductance (K_x) under scenarios in which (1) collapse induces 30–70% reduction of cross-sectional conductivities (K_t) in minor veins (black crosses); (2) collapse induces 90–99% reduction of K_t in minor and third-order veins (gray triangles). White circles are results from simulations in which no collapse occurs, and the largest conduits in the midrib embolize first. Model inputs can be found in Supporting Information Table S2. The solid line in both left and right panels represents the maximum likelihood function that best fitted the measured percentage loss of xylem hydraulic conductance. The gray vertical line represents the leaf bulk turgor loss point.

across all species, the largest conduits were located closest to the pith, with small and packed tracheids occurring more often towards the outer xylem, close to the phloem (Figs S2, S3).

Finally, although embolisms first form in the petiole and midrib in *C. diversifolia*, it is the high percentage of embolized conduits in the second- and third-order veins at strong tensions (<−6 MPa) that seem to be driving the decline in K_x in that species; that effect would likely be even stronger if data were available to simulate K_x decline driven by embolism in the largest conduits embolizing first, rather than assuming equally sized conduits in those two vein orders.

Leaf veins in the context of the hydraulic vulnerability segmentation hypothesis

The finding that embolism initiates in petiole and midrib conduits, and not in minor veins, was at first sight rather surprising. Minor veins would experience greater tensions during transpiration, as they are located at the end of the plant xylem pathway, and are thus more likely to reach air-seeding pressures. However, minor vein conduits also are much narrower than xylem conduits in the major veins, and would better resist air-seeding at any given tensions (Sack & Scoffoni, 2013), if air seeding pressure relates to a ‘rare pit’ of high vulnerability, given that narrower conduits have less wall surface area and thus fewer such rare pits (Christman *et al.*, 2009, 2012). Further, these results suggest that the hydraulic vulnerability segmentation hypothesis (Tyree & Ewers, 1991), which predicts that the most distal parts of the xylem pathways should be most vulnerable to protect the basal portions from hydraulic failure, would not hold within the leaf. However, minor veins are not the most distal segment of the whole leaf hydraulic network: the outside-xylem pathways hold that distinction. In light of our results, we propose that hydraulic vulnerability segmentation would be achieved at the whole leaf scale by having outside-xylem pathways that are even more vulnerable than either major or minor veins. There may be no advantage for leaves to have minor veins more vulnerable to drought-induced embolism than major veins, for at least three reasons. First, because of high conduit redundancy in major veins, even with a high degree of embolism in these vein orders, water could still potentially flow through the remaining functional conduits and reach the minor veins and mesophyll during drought (Brodribb *et al.*, 2016b). Second, during extreme drought, a high degree of petiole or midrib embolism could potentially isolate the entire leaf from the plant network, reducing plant water loss. Third, refilling a large petiole or midrib vessel would have a greater impact towards restoring hydraulic function than refilling smaller conduits in minor veins. Because our microCT measurements were performed on leaves from detached shoots, it is possible that midrib and petiole embolism was enhanced by air-seeding from open conduits at the cut end of the shoot, although such a scenario was unlikely as few to no conduits extended from the stem into the leaf in our four species (Scoffoni & Sack, 2015). MicroCT imaging performed on leaves in intact grapevine plants revealed similar patterns to our findings (i.e. that embolism initiates in midrib conduits rather than in higher order veins; C. Albuquerque & A. J. McElrone, pers. comm.).

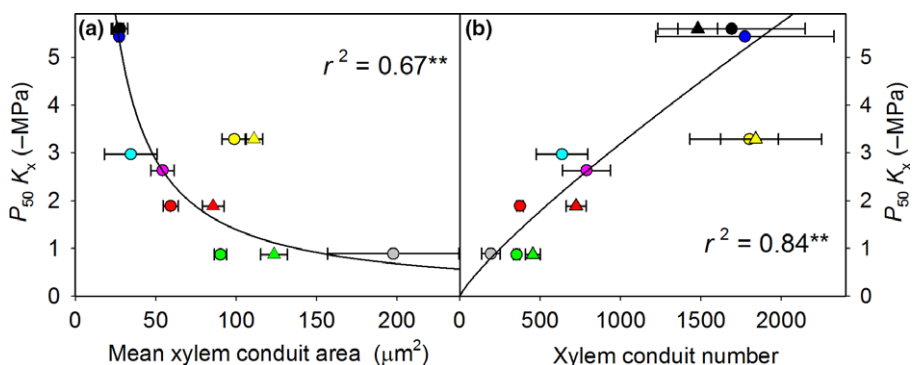


Fig. 12 The water potential at 50% loss of xylem hydraulic conductance ($P_{50}K_x$) plotted against (a) the average xylem conduit cross-sectional area (A_{mid}) and (b) the number of conduits (N_{Cmid}) in the midribs (circles) and petioles (triangles) of the study species. *Cercocarpus betuloides* (light blue); *Comarostaphylis diversifolia* (black); *Hedera canariensis* (red); *Lantana camara* (green); *Magnolia grandiflora* (yellow); *Malosma laurina* (purple); *Quercus agrifolia* (dark blue); *Salvia canariensis* (gray). Standard major axes were fitted through log-transformed values to estimate power law relationships for midrib values only: $P_{50}K_x = 154 \times A_{\text{mid}}^{-1.02}$; $P_{50}K_x = 0.01 \times N_{\text{Cmid}}^{0.84}$; **, $P < 0.01$. Error bars indicate $\pm \text{SE}$.

Our findings of earlier embolism in petiole and midrib than higher order veins contrast at first sight with those of dye uptake studies from more than a decade ago (Salleo *et al.*, 2001; Nardini *et al.*, 2003; Trifilo *et al.*, 2003a,b). Those studies provided dye solution to leaves conducting transpiration or under partial vacuum and concluded that minor veins were embolizing before major veins during leaf dehydration because dye did not apparently reach those vein orders under high tensions. We propose that the lack of minor vein dye uptake in those studies was either due to strong decreases of outside-xylem hydraulic conductance at these water potentials, which would decrease the flow rate of water through the leaf, or due to highly embolized petioles preventing dye from reaching minor veins. Several recent studies agree with our findings that conduits in the midribs embolize before minor veins. A modelling study showed that embolism in the midrib would have a stronger effect in reducing K_x than embolism in higher order veins, given the high length per area of higher order veins (McKown *et al.*, 2010). Second, studies using either optical visualization of embolism or neutron imaging of excised leaves showed that embolism appears to be more common in the midrib before spreading to higher order veins (Defraeye *et al.*, 2014; Brodribb *et al.*, 2016b).

No significant impact of conduit collapse on K_x decline

Our model simulations showed xylem conduit collapse of minor and third-order veins would have little impact on the decline of K_x with dehydration if such a phenomenon does occur in angiosperm leaf veins. Xylem conduit collapse has been observed thus far only in needles of pine species (Cochard *et al.*, 2004a) and needles of pine seedlings which possessed very low tracheid thickness to span ratio (Bouche *et al.*, 2016). Collapse of xylem conduits in midribs of angiosperms was not observed using cryo-scanning electron microscopy on leaf sections even under high levels of dehydration (Johnson *et al.*, 2009), and studies of minor vein anatomy have concluded these are overbuilt to resist collapse (Blackman *et al.*, 2010). However, more studies of potential vein collapse are needed on a wider set of species, especially species with soft leaves that would undergo strong shrinkage with

dehydration. Regardless of whether or not collapse occurs in some angiosperm leaves, our model simulations suggested that these would have very little influence on the decline of K_x with dehydration.

Evidence of embolism initiating from *de-novo* air-seeding

MicroCT imaging also provided new evidence for the connectivity of embolized conduits within leaf veins. We found that most embolized conduits were highly interconnected, although a few embolized conduits in the petiole and veins were isolated from other embolized conduits. These results are consistent with a previous study using optical visualization in leaves, and microCT studies on stems showing similar patterns (Choat *et al.*, 2015, 2016; Knipfer *et al.*, 2015a; Brodribb *et al.*, 2016b), all suggesting that air-seeding from empty conduits acts as the principal mechanism for the spread of embolism in leaf veins, although the occurrence of some isolated embolized conduits suggests that embolism can initiate from *de novo* air-seeding (Choat *et al.*, 2015; Knipfer *et al.*, 2015a). The spread of embolism could potentially relate to defects in the secondary xylem wall during development, nucleation from hydrophobic surfaces (Tyree *et al.*, 1994), homogeneous nucleation (Pickard, 1981) and/or, according to recent hypotheses for the importance of nanobubbles, a low amount (or decrease) of surfactants that would stabilize nanobubbles in the xylem sap of the particular conduit (Jansen & Schenk, 2015; Schenk *et al.*, 2015; Vera *et al.*, 2016).

Independence of vein size and vulnerability to embolism

A previous study using the optical method found embolism occurred first in lower order veins for given leaves, and that it apparently occurred first in larger diameter veins across four species from very distantly related lineages (*Adiantum capillus-veneris*, *Eucalyptus globulus*, *Pteris cretica* and *Quercus robur*, Brodribb *et al.*, 2016b). Those findings were interpreted as supporting a general scaling of vein diameter with conduit average diameter within the vein across species, and thus that vein diameter could predict susceptibility to embolism within

leaves and across species (Brodribb *et al.*, 2016b). Although our findings support and demonstrate directly that larger conduit size can explain embolism probability across species, we found no significant correlation between petiole and midrib diameters with xylem hydraulic vulnerability across our eight diverse angiosperm species. Although a scaling of midrib width with conduit size would be expected across closely related species (Coomes *et al.*, 2008), it is unlikely to hold across diverse species and lineages which would differ widely in other anatomical traits (such as pit structure) and ecological adaptation. Instead, our results showed a significant impact of the internal vein structure – that is, of conduit dimensions within the petiole and midrib—on xylem hydraulic vulnerability. Our finding that species with smaller conduit sizes and higher redundancy of xylem conduits in the midrib and petiole tended to be more resistant to K_x decline is analogous to the pattern observed for the stem xylem (Hargrave *et al.*, 1994; Ewers *et al.*, 2007; Cai & Tyree, 2010). The correlation between midrib xylem conduit diameter and xylem hydraulic vulnerability was nonlinear, as expected given that species could achieve greater resistance to hydraulic decline through other mechanisms than conduit dimensions. Although it seems improbable a species could evolve large conduit dimensions and be highly resistant to K_x decline, small conduit sizes could evolve in species exhibiting both high and low vulnerability to drought-induce embolism (Gleason *et al.*, 2016). Brodribb *et al.* (2016b) reported very narrow conduit sizes in the midrib of the fern *Adiantum capillus-veneris*, which was extremely sensitive to drought-induced embolism, such that initialization occurred after only 30 min of bench drying of the shoot and which had very thick midribs. The high susceptibility to drought-induced embolism of these narrow conduits could be due to larger pit pores and membranes vulnerabilities to air-seeding, as previously shown in fern stipes, and which has been interpreted as compensating for the low hydraulic efficiency conferred by their narrow xylem conduits (Brodersen *et al.*, 2014).

Future directions

Our findings provide new resolution of the onset, progress and mechanism for xylem hydraulic failure in leaves, revealing the important role of vein hierarchy and conduit dimensions on xylem susceptibility to drought-induced embolism and loss of K_x . Our results also point to the potential importance of additional anatomical factors, such as conduit lengths and pit structures, which could strongly shape species vulnerabilities to embolism. There is a surprising lack of information on conduit lengths, pit membranes and pit pore dimensions in leaf veins and how/if these differ across vein orders and species. Future work will be needed to elucidate their roles, which could be fundamental as shown for stems (Choat *et al.*, 2008). Full clarification of the internal structure not only of veins but of conduits within veins will enable a comprehensive quantitative understanding of species differences in leaf xylem hydraulic vulnerabilities and their role in providing tolerance to drought-induced hydraulic failure.

Acknowledgements

We thank the Advanced Light Source in Berkeley, California (Beamline 8.3.2) and Dula Parkinson for technical assistance. C.S. acknowledges Timothy Brodribb, Brendan Choat, Steven Jansen and Rozenn Le Hir for helpful discussion during the preparation of the manuscript. This work was supported by the US National Science Foundation (Award nos. 1146514 and 1457279), the Australian Research Council (DP150103863 and LP130101183), USDAARS Current Research Information System-5306 21220-004-00, CAPES/Brazil, and grants from NIFA Specialty Crops Research Initiative and from the American Vineyard Foundation. The Advanced Light Source is supported by the Director, Office of Science, Office of Basic Energy Sciences, of the US Department of Energy under Contract no. DE-AC02-05CH11231.

Author contributions

C.S., C.R.B., A.J.M., H.C., T.N.B. and L.S. designed experiments; C.S., C.A., S.V.T., G.P.J. and A.J.M. performed experiments and simulations; C.S., C.A. and C.R.B. analyzed data; and C.S. and L.S. wrote the manuscript with contributions from all authors.

References

- Blackman CJ, Brodribb TJ, Jordan GJ. 2010. Leaf hydraulic vulnerability is related to conduit dimensions and drought resistance across a diverse range of woody angiosperms. *New Phytologist* 188: 1113–1123.
- Bouche PS, Delzon S, Choat B, Badel E, Brodribb T, Burlett R, Cochard H, Charra-Vaskou K, Lavigne B, Shan L *et al.* 2016. Are needles of *Pinus pinaster* more vulnerable to xylem embolism than branches? New insights from X-ray computed tomography. *Plant, Cell & Environment* 39: 860–870.
- Brodersen C, Jansen S, Choat B, Rico C, Pittermann J. 2014. Cavitation resistance in seedless vascular plants: the structure and function of interconduit pit membranes. *Plant Physiology* 165: 895–904.
- Brodersen CR, McElrone AJ, Choat B, Lee EF, Shackel KA, Matthews MA. 2013. *In vivo* visualizations of drought-induced embolism spread in *Vitis vinifera*. *Plant Physiology* 161: 1820–1829.
- Brodribb TJ, Bieniaime D, Marmottant P. 2016b. Revealing catastrophic failure of leaf networks under stress. *Proceedings of the National Academy of Sciences, USA* 113: 4865–4869.
- Brodribb TJ, Holbrook NM. 2005. Water stress deforms tracheids peripheral to the leaf vein of a tropical conifer. *Plant Physiology* 137: 1139–1146.
- Brodribb T, Skelton RP, McAdam SAM, Bieniaime D, Lucani CJ, Marmottant P. 2016a. Visual quantification of embolism reveals leaf vulnerability to hydraulic failure. *New Phytologist* 209: 1403–1409.
- Bucci SJ, Scholz FG, Campanello PI, Montti L, Jimenez-Castillo M, Rockwell FA, La Manna L, Guerra P, Lopez Bernal P, Troncoso O *et al.* 2012. Hydraulic differences along the water transport system of South American *Nothofagus* species: do leaves protect the stem functionality? *Tree Physiology* 32: 880–893.
- Burnham KP, Anderson DR. 2004. Multimodel inference – understanding AIC and BIC in model selection. *Sociological Methods & Research* 33: 261–304.
- Cai J, Tyree MT. 2010. The impact of vessel size on vulnerability curves: data and models for within-species variability in saplings of aspen, *Populus tremuloides* Michx. *Plant, Cell & Environment* 33: 1059–1069.
- Choat B, Badel E, Burlett R, Delzon S, Cochard H, Jansen S. 2016. Non-invasive measurement of vulnerability to drought induced embolism by X-ray microtomography. *Plant Physiology* 170: 273–282.

- Choat B, Brodersen CR, McElrone AJ. 2015. Synchrotron X-ray microtomography of xylem embolism in *Sequoia sempervirens* saplings during cycles of drought and recovery. *New Phytologist* 205: 1095–1105.
- Choat B, Cobb AR, Jansen S. 2008. Structure and function of bordered pits: new discoveries and impacts on whole-plant hydraulic function. *New Phytologist* 177: 608–625.
- Christman MA, Sperry JS, Adler FR. 2009. Testing the ‘rare pit’ hypothesis for xylem cavitation resistance in three species of *Acer*. *New Phytologist* 182: 664–674.
- Christman MA, Sperry JS, Smith DD. 2012. Rare pits, large vessels and extreme vulnerability to cavitation in a ring-porous tree species. *New Phytologist* 193: 713–720.
- Cochard H, Froux F, Mayr FFS, Coutand C. 2004a. Xylem wall collapse in water-stressed pine needles. *Plant Physiology* 134: 401–408.
- Cochard H, Nardini A, Coll L. 2004b. Hydraulic architecture of leaf blades: where is the main resistance? *Plant, Cell & Environment* 27: 1257–1267.
- Cochard H, Tyree MT. 1990. Xylem dysfunction in *Quercus* – vessel sizes, tyloses, cavitation and seasonal changes in embolism. *Tree Physiology* 6: 393–407.
- Coomes DA, Heathcote S, Godfrey ER, Shepherd JJ, Sack L. 2008. Scaling of xylem vessels and veins within the leaves of oak species. *Biology Letters* 4: 302–306.
- Defraeye T, Derome D, Aregawi W, Cantré D, Hartmann S, Lehmann E, Carmeliet J, Voisard F, Verboven P, Nicolai B. 2014. Quantitative neutron imaging of water distribution, venation network and sap flow in leaves. *Planta* 240: 423–436.
- Ewers FW, Ewers JM, Jacobsen AL, Lopez-Portillo J. 2007. Vessel redundancy: modeling safety in numbers. *Iowa Journal* 28: 373–388.
- Gleason SM, Westoby M, Jansen S, Choat B, Hacke UG, Pratt RB, Bhaskar R, Brodribb TJ, Bucci SJ, Cao K-F et al. 2016. Weak tradeoff between xylem safety and xylem-specific hydraulic efficiency across the world’s woody plant species. *New Phytologist* 209: 123–136.
- Hales S. 1727. *Vegetable staticks*. London, UK: Oldbourne Book Co.
- Hargrave KR, Kolb KJ, Ewers FW, Davis SD. 1994. Conduit diameter and drought-induced embolism in *Salvia mellifera* Greene (Labiatae). *New Phytologist* 126: 695–705.
- Jansen S, Schenk HJ. 2015. On the ascent of sap in the presence of bubbles. *American Journal of Botany* 102: 1561–1563.
- John GP, Scoffoni C, Sack L. 2013. Allometry of cells and tissues within leaves. *American Journal of Botany* 100: 1936–1948.
- Johnson DM, Meinzer FC, Woodruff DR, McCulloh KA. 2009. Leaf xylem embolism, detected acoustically and by cryo-SEM, corresponds to decreases in leaf hydraulic conductance in four evergreen species. *Plant, Cell & Environment* 32: 828–836.
- Knipfer T, Brodersen CR, Zedan A, Kluepfel DA, McElrone AJ. 2015a. Patterns of drought-induced embolism formation and spread in living walnut saplings visualized using X-ray microtomography. *Tree Physiology* 35: 744–755.
- Knipfer T, Eustis A, Brodersen C, Walker AM, McElrone AJ. 2015b. Grapevine species from varied native habitats exhibit differences in embolism formation/repair associated with leaf gas exchange and root pressure. *Plant, Cell & Environment* 38: 1503–1513.
- Lewis AM, Boose ER. 1995. Estimating volume flow-rates through xylem conduits. *American Journal of Botany* 82: 1112–1116.
- Li S, Lens F, Espino S, Karimi Z, Klepsch M, Schenk HJ, Schmitt M, Schultdt B, Jansen S. 2016. Intervessel pit membrane thickness as a key determinant of embolism resistance in angiosperm xylem. *International Association of Wood Anatomists Journal* 37: 152–171.
- McKown AD, Cochard H, Sack L. 2010. Decoding leaf hydraulics with a spatially explicit model: principles of venation architecture and implications for its evolution. *The American Naturalist* 175: 447–460.
- Nardini A, Salleo S, Raimondo F. 2003. Changes in leaf hydraulic conductance correlate with leaf vein embolism in *Cercis siliquastrum* L. *Trees-Structure and Function* 17: 529–534.
- Pickard WF. 1981. The ascent of sap in plants. *Progress in Biophysics & Molecular Biology* 37: 181–229.
- Pivovaroff AL, Sack L, Santiago LS. 2014. Coordination of stem and leaf hydraulic conductance in southern California shrubs: a test of the hydraulic segmentation hypothesis. *New Phytologist* 203: 842–850.
- Sack L, Cowan PD, Jaikumar N, Holbrook NM. 2003. The ‘hydrology’ of leaves: co-ordination of structure and function in temperate woody species. *Plant, Cell & Environment* 26: 1343–1356.
- Sack L, Holbrook NM. 2006. Leaf hydraulics. *Annual Review of Plant Biology* 57: 361–381.
- Sack L, Melcher PJ, Zwieniecki MA, Holbrook NM. 2002. The hydraulic conductance of the angiosperm leaf lamina: a comparison of three measurement methods. *Journal of Experimental Botany* 53: 2177–2184.
- Sack L, Scoffoni C. 2013. Leaf venation: structure, function, development, evolution, ecology and applications in past, present and future. *New Phytologist* 198: 938–1000.
- Salisbury EJ. 1913. The determining factors in petiolar structure. *New Phytologist* 12: 281–289.
- Salleo S, Lo Gullo MA, Raimondo F, Nardini A. 2001. Vulnerability to cavitation of leaf minor veins: any impact on leaf gas exchange? *Plant, Cell & Environment* 24: 851–859.
- Schenk HJ, Steppé K, Jansen S. 2015. Nanobubbles: a new paradigm for air-seeding in xylem. *Trends in Plant Science* 20: 199–205.
- Scoffoni C, Jansen S. 2016. I can see clearly now – embolisms in leaf veins. *Trends in Plant Science* 21: 723–725.
- Scoffoni C, McKown AD, Rawls M, Sack L. 2012. Dynamics of leaf hydraulic conductance with water status: quantification and analysis of species differences under steady-state. *Journal of Experimental Botany* 63: 643–658.
- Scoffoni C, Rawls M, McKown A, Cochard H, Sack L. 2011. Decline of leaf hydraulic conductance with dehydration: relationship to leaf size and venation architecture. *Plant Physiology* 156: 832–843.
- Scoffoni C, Sack L. 2015. Are leaves “freewheelin’”? Testing for a Wheeler-type effect in leaf xylem hydraulic decline. *Plant, Cell & Environment* 38: 534–543.
- Scoffoni C, Vuong C, Diep S, Cochard H, Sack L. 2014. Leaf shrinkage with dehydration: coordination with hydraulic vulnerability and drought tolerance. *Plant Physiology* 164: 1772–1788.
- Sheffield J, Wood EF. 2008. Projected changes in drought occurrence under future global warming from multi-model, multi-scenario, IPCC AR4 simulations. *Climate Dynamics* 31: 79–105.
- Taneda H, Terashima I. 2012. Co-ordinated development of the leaf midrib xylem with the lamina in *Nicotiana tabacum*. *Annals of Botany* 110: 35–45.
- Trifilo P, Gasco A, Raimondo F, Nardini A, Salleo S. 2003a. Kinetics of recovery of leaf hydraulic conductance and vein functionality from cavitation-induced embolism in sunflower. *Journal of Experimental Botany* 54: 2323–2330.
- Trifilo P, Nardini A, Lo Gullo MA, Salleo S. 2003b. Vein cavitation and stomatal behaviour of sunflower (*Helianthus annuus*) leaves under water limitation. *Physiologia Plantarum* 119: 409–417.
- Trifilo P, Raimondo F, Savi T, Lo Gullo MA, Nardini A. 2016. The contribution of vascular and extra-vascular water pathways to drought-induced decline of leaf hydraulic conductance. *Journal of Experimental Botany* 67: 4917–4919.
- Tyree MT, Davis SD, Cochard H. 1994. Biophysical perspectives of xylem evolution: is there a tradeoff of hydraulic efficiency for vulnerability to dysfunction. *Iowa Journal* 15: 335–360.
- Tyree MT, Ewers FW. 1991. The hydraulic architecture of trees and other woody-plants. *New Phytologist* 119: 345–360.
- Vera F, Rivera R, Romero-Maltrana D, Villanueva J. 2016. Negative pressures and the first water siphon taller than 10.33 meters. *PLoS ONE* 11: e0153055.
- Warton DI, Wright IJ, Falster DS, Westoby M. 2006. Bivariate line-fitting methods for allometry. *Biological Reviews* 81: 259–291.
- Weast RC. 1974. *Handbook of chemistry and physics*, 54th edn. Cleveland, OH, USA: CRC Press.
- Xiao X, White EP, Hooten MB, Durham SL. 2011. On the use of log-transformation vs. nonlinear regression for analyzing biological power laws. *Ecology* 92: 1887–1894.
- Yang SD, Tyree MT. 1993. Hydraulic resistance in *Acer saccharum* shoots and its influence on leaf water potential and transpiration. *Tree Physiology* 12: 231–242.
- Zhang Y-J, Rockwell FE, Wheeler JK, Holbrook NM. 2014. Reversible deformation of transverse tracheids in *Taxus baccata* is associated with a reversible decrease in leaf hydraulic conductance. *Plant Physiology* 165: 1557–1565.

Supporting Information

Additional Supporting Information may be found online in the Supporting Information tab for this article:

Fig. S1 Histograms of midrib and petiole conduit diameter classes across the eight study species.

Fig. S2 Histograms of minor vein conduit diameter classes across the eight study species.

Fig. S3 Midrib diameter is independent from its mean conduit size and number across eight diverse species in phylogeny and drought tolerance.

Methods S1 Leaf xylem hydraulic vulnerability curves using the vacuum pump method and X-ray micro-computed tomography imaging.

Table S1 Mean conduit diameter in the petiole, midrib and minor veins for the eight study species, measured from light microscopy sections

Table S2 K_{LEAF} inputs of the simulation of the influence of embolism on leaf xylem hydraulic conductance

Table S3 K_{LEAF} inputs of the simulation of the influence of xylem collapse on leaf xylem hydraulic conductance

Please note: Wiley Blackwell are not responsible for the content or functionality of any Supporting Information supplied by the authors. Any queries (other than missing material) should be directed to the *New Phytologist* Central Office.



About New Phytologist

- *New Phytologist* is an electronic (online-only) journal owned by the New Phytologist Trust, a **not-for-profit organization** dedicated to the promotion of plant science, facilitating projects from symposia to free access for our Tansley reviews.
- Regular papers, Letters, Research reviews, Rapid reports and both Modelling/Theory and Methods papers are encouraged. We are committed to rapid processing, from online submission through to publication 'as ready' via *Early View* – our average time to decision is <28 days. There are **no page or colour charges** and a PDF version will be provided for each article.
- The journal is available online at Wiley Online Library. Visit www.newphytologist.com to search the articles and register for table of contents email alerts.
- If you have any questions, do get in touch with Central Office (np-centraloffice@lancaster.ac.uk) or, if it is more convenient, our USA Office (np-usaoffice@lancaster.ac.uk)
- For submission instructions, subscription and all the latest information visit www.newphytologist.com